Wood Sci Technol (2014) 48:755–772
DOI 10.1007/s00226-014-0638-z

ORIGINAL

Development of constitutive model for laminated veneer lumber using digital image correlation technique

W. A. van Beerschoten · D. M. Carradine · A. Carr

Received: 20 June 2013 / Published online: 17 May 2014

Abstract This paper describes the development of a three-dimensional constitutive model for laminated veneer lumber (LVL) needed for new developments using this material. The LVL was manufactured in New Zealand from Radiata Pine. Experimental testing has been performed according to European timber testing standards. Block compression testing has resulted in modulus of elasticity values in the three material directions. Digital image correlation (DIC) technique has been used to determine the six Poisson's ratios. Shear testing, whereby timber specimens were glued between two steel plates, has given stiffness values using DIC measurements. Experimental testing results have been compared with values found in literature. Results from this experimental testing programme have made it possible to create a three-dimensional elastic material model of LVL for the use in finite element analysis programmes. Although the material properties do not result in a symmetrical constitutive matrix, only minor adjustments are needed to gain the benefits of a symmetrical matrix.

Introduction

Timber is an orthotropic material, which means that material properties vary depending upon the orientation. Being a naturally grown product, there are numerous factors which influence the strength and stiffness, resulting in significant variability of material properties. Laminated veneer lumber (LVL) has the

W. A. van Beerschoten (✉) · A. Carr
University of Canterbury, Private Bag 4800, Christchurch 8140, New Zealand
e-mail: wav13@uclive.ac.nz

D. M. Carradine
BRANZ, Private Bag 50908, Porirua City 5240, New Zealand

advantage that defects are distributed, making the material properties relatively homogeneous compared to sawn timber (Buchanan 2007).

New developments in the field of structural timber engineering, such as post-tensioned timber construction (Buchanan et al. 2011; Palermo et al. 2005) with complex connection behaviour (van Beerschoten et al. 2011a, b), require three-dimensional (3D) finite element modelling (FEM). To get reliable results from these models, it is necessary to have an accurate material definition to form the constitutive matrix. This material model consists of three moduli of elasticity (E), three Poisson's ratios (v) and three shear moduli (G).

The first publications on elastic properties in timber date back to the early twentieth century, of which an overview table is published in Hearmon (1948). Other publications on elastic constants of wood from similar time refer to these initial tests (U.S. Department of Agriculture Forest Products Laboratory 1955; Wangaard 1950). Later publications introduce different test methods for determination of elastic properties. Gunnerson et al. (1973) described a plate testing method using two-way bending, which is concluded to be a good technique to determine elastic properties, but problems arise in calculation of Poisson's ratios as small deflections cannot be measured accurately enough. Bodig and Goodman (1973) used this technique and compression testing. Their publication contains an extensive list of elastic properties of different timber species, including numerous pine species. A more recent publication (Bucur 2006) describes ultrasonic techniques which can be used in nondestructive testing. This method is compared with static compression testing by Goncalves et al. (2011). The only values for LVL have been found in a publication by Janowiak et al. (2001), where several elastic properties of three types of LVL have been evaluated. An overview of elastic properties found in literature is provided in Table 1.

Worldwide, there are a number of testing standards to determine mechanical properties of timber. These standards usually specify bending, compression or tensile tests for evaluation of modulus of elasticity. Shear modulus is often specified based on bending tests (single span or variable span), torsion tests and more recently shear field tests (EN 408 2010). No timber testing standard specifies tests for Poisson's ratio, but ASTM E132-04 (2010) specifies a general test method for determination of Poisson's ratio using extensometers during tension tests of structural materials.

In literature, several methods for determining Poisson's ratios can be found. Early publications on Poisson's ratios in timber (Hearmon 1948) do not describe exact testing procedures except that testing was carried out using large-scale testing machinery. Sliker (1972) described a method using small strips of timber (32 in. $\times$ 3.5 in. $\times$ 0.25 in.) in a testing machine with bonded electrical-resistance strain gages mounted in a rectangular pattern in the centre of the specimen. Results were consistent with a small variation, but only two material directions have been tested. Zink et al. (1997) published the use of digital image correlation (DIC) technique using white light speckle technique on compression specimens. This technique allowed multiple measurements spanning the entire specimen rather than from one or two points per specimen. This technique proved successful and the authors discovered that the Poisson's ratios are not constant during testing, but decrease with increasing load.

Table 1 Timber material properties from literature and experimental testing

Author	Timber species	E_L	E_T	E_R	ν_{LT}	ν_{TL}	ν_{LR}	ν_{RL}	ν_{TR}	ν_{RT}	G_{LT}	G_{LR}	G_{TR}
Experimental testing	Radiata pine LVL	12,157	426	371	0.59	0.02	0.48	0.02	0.22	0.14	856	901	96
Hearmon (1948)	Scots pine	16,300	570	1,100	0.51	0.015	0.42	0.038	0.31	0.68	680	1,160	66
	Softwoods (min. values)	10,700	430	710	0.37	0.015	0.37	0.028	0.25	0.43	620	500	23
	Softwood (max. values)	16,400	900	1,300	0.51	0.025	0.43	0.038	0.40	0.68	910	1,180	79
	Hardwoods (min. values)	10,200	510	1,130	0.43	0.009	0.23	0.018	0.24	0.60	600	900	190
	Hardwoods (max. values)	16,300	1140	2,240	0.64	0.044	0.49	0.073	0.38	0.78	1,060	1,610	460
U.S. Dep. of Agriculture Forest Prod. Lab. (1955)	Walnut	12,741	714	1,351	0.632	0.036	0.495	0.052	0.367	0.718	790	1,083	266
	Yellow-Poplar	11,983	515	1102	0.392	0.019	0.318	0.03	0.329	0.703	827	899	132
Bodig and Goodman (1973)[a]	Sugar pine	6,743	588	884	0.349	–	0.356	–	0.358	0.428	763	836	96
	West. white pine	9,273	352	728	0.344	–	0.329	–	0.334	0.410	443	478	49
	Ponderosa pine	7,729	642	946	0.400	–	0.337	–	0.359	0.426	887	1,069	117
	Lodgepole pine	6,557	447	666	0.347	–	0.316	–	0.381	0.469	301	322	32
	Red pine	9,873	430	867	0.315	–	0.347	–	0.308	0.408	800	945	114
	Loblolly pine	11,087	871	1,253	0.292	–	0.328	–	0.362	0.382	898	903	142
	Pond pine	19,036	781	1,356	0.364	–	0.280	–	0.320	0.389	862	958	173
	Longleaf pine	14,644	805	1,487	0.365	–	0.332	–	0.342	0.384	886	1038	172
	Slash pine	15,975	725	1,189	0.444	–	0.392	–	0.387	0.447	843	883	157
Forest Products Lab. (1979)	Douglas fir	13,400	670	911	0.45	0.02	0.29	0.02	0.29	0.39	1045	858	94
Bucur (2006)[b]	Sitks spruce	9,564	487	1,037	0.45	0.49	0.43	–	–	–	1,095	1,196	91
Goncalves et al. (2011)[c]	Blue gum	13,617	2,180	3680	0.78	0.060	0.333	0.038	0.300	0.420	1172	2360	829
	Garapeira	14,333	1,452	2,323	0.250	0.078	0.180	0.040	0.330	0.790	1,489	1,865	536
Janowiak et al. (2001)[d]	Southern pine LVL	16,500	580	–	0.644	–	–	–	–	–	476	354	64
	Douglas fir LVL	18,300	500	–	0.580	–	–	–	–	–	405	331	46
	Yellow-Poplar LVL	15,200	450	–	0.604	–	–	–	–	–	247	314	96

[a] Values converted from psi to MPa

[b] Using acoustic testing methods

[c] Average values taken from static testing

[d] Poisson's ratios taken from compression test and shear values taken from five-point bending test

A similar technique was used by Ling et al. (2009), whereby stochastic neural networks were used to approximate the displacement profiles. Niemz and Caduff (2008) have determined the Poisson's ratios of spruce using a specially fabricated testing machine, capable of measuring transversal deformations with an accuracy of 0.0015 mm. They tested 20 samples for each of the three different orientations. Results were in line with literature values, and variations between 17 and 62 % were found between measurements. Another publication (Garab et al. 2010) used DIC for determining the Poisson's ratios under seven different growth ring angles, whereby a total of 182 specimens were tested. A video system recorded a 10×10 mm^2 section with a resolution of 950×950 pixels and used this to create full-field displacement profiles, resulting in low coefficient of variations (7–19 %).

There have been numerous publications on shear tests focussing on shear strength of timber, i.e. Denzler and Glos (2007). The number of papers focussing on shear stiffness is limited, though several testing methods are published. Vibration time measurements have been used to determine the shear modulus of glulam beams (Görlacher and Kürth 1994). Divos et al. (1998) compared a static three-point deflection method with vibrational methods and concluded that static and torsional vibration methods are good, but the vibration method is more precise. A new block shear test (Sretenovic et al. 2004), whereby the specimen was glued between two sections of beech, gave promising results and, in comparison with ASTM D143 2009 block test, showed a more uniform shear field. Another method, similar to the ASTM test setup, was proposed by Ukyo et al. (2010), and the DIC technique has been used to evaluate the shear modulus. A similar technique (digital speckle photography) has been used by Hassel et al. (2009), but this time on small square blocks, making it possible to test different material orientations, although only the rolling shear modulus has been tested. Brandner et al. (2008) used shear field measurements during standard four-point bending tests. This procedure integrates determination of shear modulus with standard testing methods. For this test method, large specimen sizes are needed, which is not a problem when glulam is used, but is problematic when analysing shear moduli in different material orientations. Dahl and Malo (2009) tested shear properties of Norway spruce using the Arcan shear test of small specimens in six different directions. Video extensometry was used to track displacements of a grid of dots on each specimen. Their test setup meant that they had to perform FEM analysis in order to derive modification factors for the shear modulus as shear stresses were not constant in the measurement area. The method published in this paper combines a standard testing method using small specimens with the use of the DIC technique to provide an easy way to measure the shear modulus in different material orientations. FEM analysis has resulted in a single factor to take the nonlinear stress distribution into account.

Digital image correlation (DIC) is a technique for measuring deformations and strains (Pan et al. 2009). Software allows users to track displacements of points through a series of images taken during the experimental testing. This technique provides full-field displacements and strains, whereas traditionally used potentiometers and strain gauges only give point wise measurements. Although DIC is widely used in the field of experimental mechanics, there is still a great potential for this technique in the field of timber testing.

This paper presents experimental results of compression and shear testing on Radiata Pine LVL, performed according to European standards EN 14374 (2004) (requirements for LVL) and EN 408 (2010) (testing methods). The latter specifies pure block compression tests and shear tests with a relatively uniform shear distribution. DIC techniques have been used to determine the material properties needed for the formation of a 3D elastic material model. A full description of the compression strength and stiffness of LVL has been published in van Beerschoten et al. (2013), and this article provides a summary of these test results.

Theory

For the development of a 3D linear finite element material model, a total of nine material properties are needed for the constitutive equations; three moduli of elasticity (E), three Poisson's ratios (v) and three shear moduli (G). These equations are shown in the form of the compliance matrix in Eq. 1. For LVL, having veneers rotary peeled and glued back together, there is no influence of growth rings and a clearly defined rectangular coordinate system can be used as shown in Fig. 1. The three material directions are (1) Longitudinal—parallel to grain; (2) Tangential—perpendicular to grain and parallel to glue lines; and (3) Radial—perpendicular to grain and perpendicular to glue lines.

$$\begin{Bmatrix} \epsilon_{11} \\ \epsilon_{22} \\ \epsilon_{33} \\ \gamma_{12} \\ \gamma_{13} \\ \gamma_{23} \end{Bmatrix} = \begin{bmatrix} \frac{1}{E_1} & \frac{-v_{21}}{E_2} & \frac{-v_{31}}{E_3} & 0 & 0 & 0 \\ \frac{-v_{12}}{E_1} & \frac{1}{E_2} & \frac{-v_{32}}{E_3} & 0 & 0 & 0 \\ \frac{-v_{13}}{E_1} & \frac{-v_{23}}{E_2} & \frac{1}{E_3} & 0 & 0 & 0 \\ 0 & 0 & 0 & \frac{1}{G_{12}} & 0 & 0 \\ 0 & 0 & 0 & 0 & \frac{1}{G_{13}} & 0 \\ 0 & 0 & 0 & 0 & 0 & \frac{1}{G_{23}} \end{bmatrix} \begin{Bmatrix} \sigma_{11} \\ \sigma_{22} \\ \sigma_{33} \\ \sigma_{12} \\ \sigma_{13} \\ \sigma_{23} \end{Bmatrix} \quad (1)$$

For an orthotropic material like timber, there are a total of six Poisson's ratios: $v_{12}, v_{13}, v_{21}, v_{23}, v_{31}, v_{32}$. Although it is commonly assumed that only three of these are independent, as finite element analysis programmes assume a symmetrical constitutive matrix. This means that off-diagonal terms have to be equal, which leads to relationships in Eq. 2. Validity of this assumption is evaluated in the discussion section of this paper.

$$\frac{v_{12}}{E_1} = \frac{v_{21}}{E_2}; \quad \frac{v_{13}}{E_1} = \frac{v_{31}}{E_3}; \quad \frac{v_{23}}{E_2} = \frac{v_{32}}{E_{23}} \quad (2)$$

Materials and methods

The LVL used for this research is manufactured from New Zealand Radiata Pine by Nelson Pine Industries Limited (2010). Specimens had a thickness of 45 mm and consisted of 13 veneers of approximately 3.5 mm thick. The material is specified as LVL11, with characteristic properties as shown in Table 2. These values are based

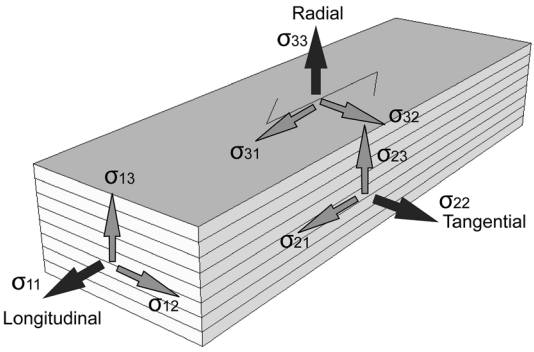

Fig. 1 Coordinate system and stress directions in LVL

Table 2 Characteristic properties of LVL11 (Nelson Pine Industries Limited 2010)

Property		Magn.	Unit
Modulus of elasticity	E	11	GPa
Bending strength	f_b	48	MPa
Compr. strength par. to grain	f_c	45	MPa
Compr. strength perp. to grain	$f_{c,90}$	12	MPa
Tensile strength par. to grain	f_t	30	MPa
Shear strength (edgewise, G_{TL})	f_s	6	MPa

on AS/NZS 4063:1992 (Standard New Zealand 1992) strength values are derived from the 5th percentile, corrected by an equation including the variability and sample size. Stiffness values are based on corrected mean values. Although values for one modulus of elasticity are given by manufacturers, this is based on four-point bending tests and include shear deformation (Nelson Pine Industries Limited 2010). Therefore, this value cannot be used for the constitutive equations. The timber was stored at ambient laboratory conditions, and density and moisture content were evaluated immediately following testing. Density was measured at an average of 581 kg/m^3 (CoV = 0.7 %) and moisture content at an average of 9.3 % (CoV = 14 %) for shear testing and 8.9 % (CoV = 7 %) for compression testing. For shear testing, a two-part epoxy (Epi-Glue) was used to fix the steel plates to the timber specimens. Pressure was applied for about 4 h while the epoxy hardened after which specimens were placed in an oven at 35 °C for the epoxy to fully cure.

Compression testing was performed using five or six replicates in the three different material directions for 45 mm thick LVL. European Standards have been used for compression testing. EN 14374 (2004) specifies requirements for LVL, although for testing it refers to methods outlined in EN 408 (2010). For parallel to grain stiffness, a small column with a height of '6 × d' (d = depth of specimen in mm) is specified. For compression perpendicular to grain, a block compression test is specified with a specimen height of 90 mm. Further specimen dimensions are given in Table 3. Testing was performed using an Instron testing frame with an in-line 150 kN load cell. Two small linear displacement potentiometers (10 mm travel)

Table 3 Specimen description and average dimensions for tested compression and shear specimens

Test	Parameters	No. of tests	Length (mm)	Depth (mm)	Height (mm)
Compr. 1	E_1, ν_{12}, ν_{13}	6	44.7	45.1	271.2
Compr. 2	E_2, ν_{21}, ν_{23}	5	71.2	45.4	89.2
Compr. 3	E_3, ν_{31}, ν_{32}	5	71.6	44.9	91.1
Shear 1	G_{12}	6	295.0	45.3	44.9
Shear 2	G_{13}	6	272.7	29.9	44.8
Shear 3	G_{21}	6	296.8	45.4	45.3
Shear 4	G_{23}	6	272.9	31.9	42.6
Shear 5	G_{31}	6	295.3	31.7	43.9
Shear 6	G_{32}	6	295.7	31.8	45.2

were placed on both sides at 20 and 80 % of the specimen height. Testing was stopped at 10 % strain deformation, as further deformation was deemed unrealistic. Stiffness is defined as the slope of load-deformation curve between 10 and 40 % of maximum load.

Shear testing was also performed according to EN 408 (2010) with six specimens for each shear direction. Testing was performed in an Avery test frame with a capacity of 100 kN whereby specimens were loaded until failure. Specimen dimensions are given in Table 3. Due to material dimensions, specimens had a depth of 45 mm instead of 55 mm as specified in EN 408 (2010). Therefore, steel side plates were manufactured with a thickness of 15 mm, 5 mm thicker than specified by the standard, in order to keep the 14° angle of the specimen. Further details of the shear testing can be found in Dunbar et al. (2011).

During compression and shear testing 18MegaPixel (5,184 × 3,456 pixels) RAW images of the specimen have been taken at intervals of 5 s using Digital SLR cameras, as shown in Fig. 2. These images have been analysed using software, a MATLAB script (developed by C. Eberl from Karlsruhe Institute of Technology, freely available for download from MATLAB Central), which was used to generate a grid of markers which were tracked through the series of images. For compression testing, 40–70 markers were placed between 20 and 80 % of the specimen height. Vertical and horizontal displacements were converted to strains and averaged for all markers. For shear testing, grids of up to 280 markers have been used.

Experimental testing

Modulus of elasticity

The modulus of elasticity (E) has been evaluated using the average displacement readings from potentiometers on both sides of the test specimen and load values from the load cell. Displacement values were divided by the distance between measuring points, and load values were divided by specimen cross-

sectional area. The modulus of elasticity has been evaluated using a trendline between 10 and 40 % of the maximum stress in the stress–strain graph. Further information about the compressive strength and stiffness can be found in van Beerschoten et al. (2013).

Poisson's ratio

The Poisson's ratios (Fig. 3a) of LVL have been evaluated from strain fields generated using DIC software. For each test, two series of images, one for each side, were taken using DSLR cameras. A virtual grid of markers was generated, as is shown in Fig. 3b. Each marker represents a square of 50 × 50 pixels which are tracked through the series of images. The coordinate of each marker is stored, and displacement relative to the first image is calculated.

Average vertical and horizontal strains, calculated from displacements, during testing are shown in Fig. 3c. Also shown in the same figure is the Poisson's ratio, with almost perfect linear behaviour after the first 5 pictures. The Poisson's ratio has been based on an average value between image number 30 and 60, whereby negative values were omitted. This range was different from the 10–40 % of maximum load which was used for evaluation of modulus of elasticity and shear modulus. During the first stage of testing, strains were too small to give reliable results and close to failure, the material behaviour was no longer linear elastic. For testing with load applied in the longitudinal direction, strain data were available from DIC and potentiometers. It was found that the measurements from potentiometers were more accurate, and therefore, this was used for evaluation of ν_{LR} and ν_{LT}. Poisson's ratios for all tests are shown in Fig. 4. It can be seen that for certain directions, especially when evaluating very small strains in grain direction (due to high E), there is a large spread in results. In several of these cases (ν_{TL} and ν_{RL}), measured displacements were less than 5 pixels, and although the software applies sub-pixel analysis techniques, this gave issues with accuracy.

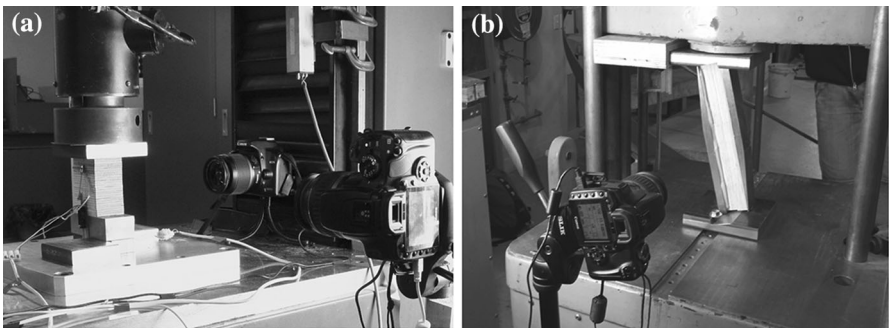

Fig. 2 Camera setup during experimental testing. **a** Compression test, **b** shear test

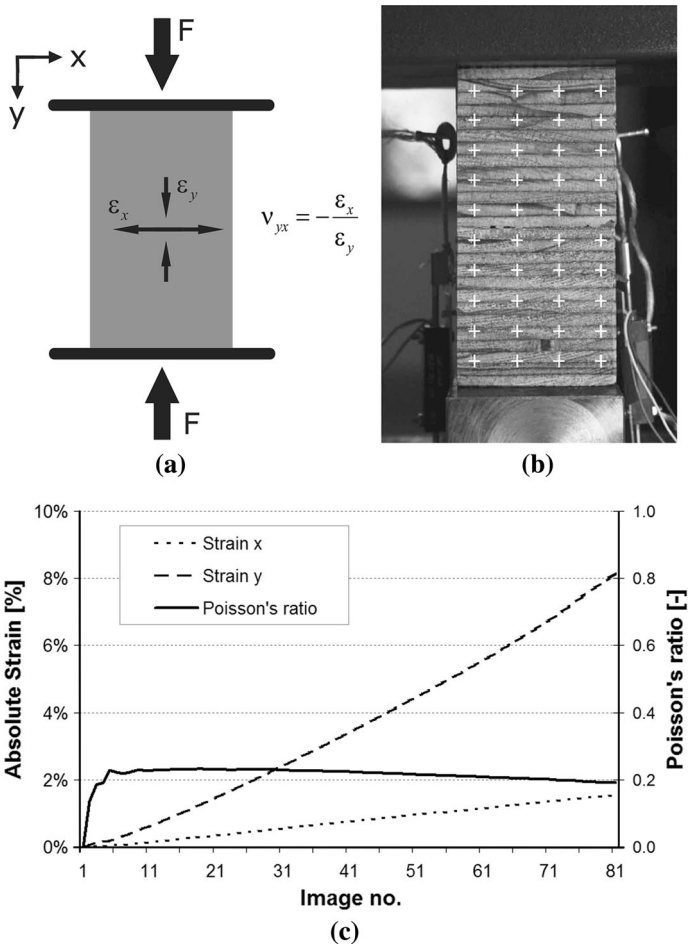

Fig. 3 Evaluation of Poisson's ratio. **a** Definition of *v*, **b** grid on specimen, **c** horizontal and vertical strain and Poisson's ratio

Modulus of rigidity

For calculation of the shear stress EN 408 (2010) specifies Eq. 3. This equation calculates the shear force and divides this over the full cross-sectional area of the specimen, assuming a constant shear distribution. This assumption has been checked using two-dimensional and three-dimensional FEM modelling. As there were only minor differences between 3D and 2D models, the 2D model (Fig. 5) is described here. For this model, steel support plates and timber have been modelled as generalised plain-strain elements. The epoxy connection between steel and timber has been modelled using tie constraints, a model with an adhesive layer included gave an almost identical shear stress distribution. Four node quadratic elements (CPEG8) have been used. Reduced integration elements (CPEG8R) were also tried and gave the same

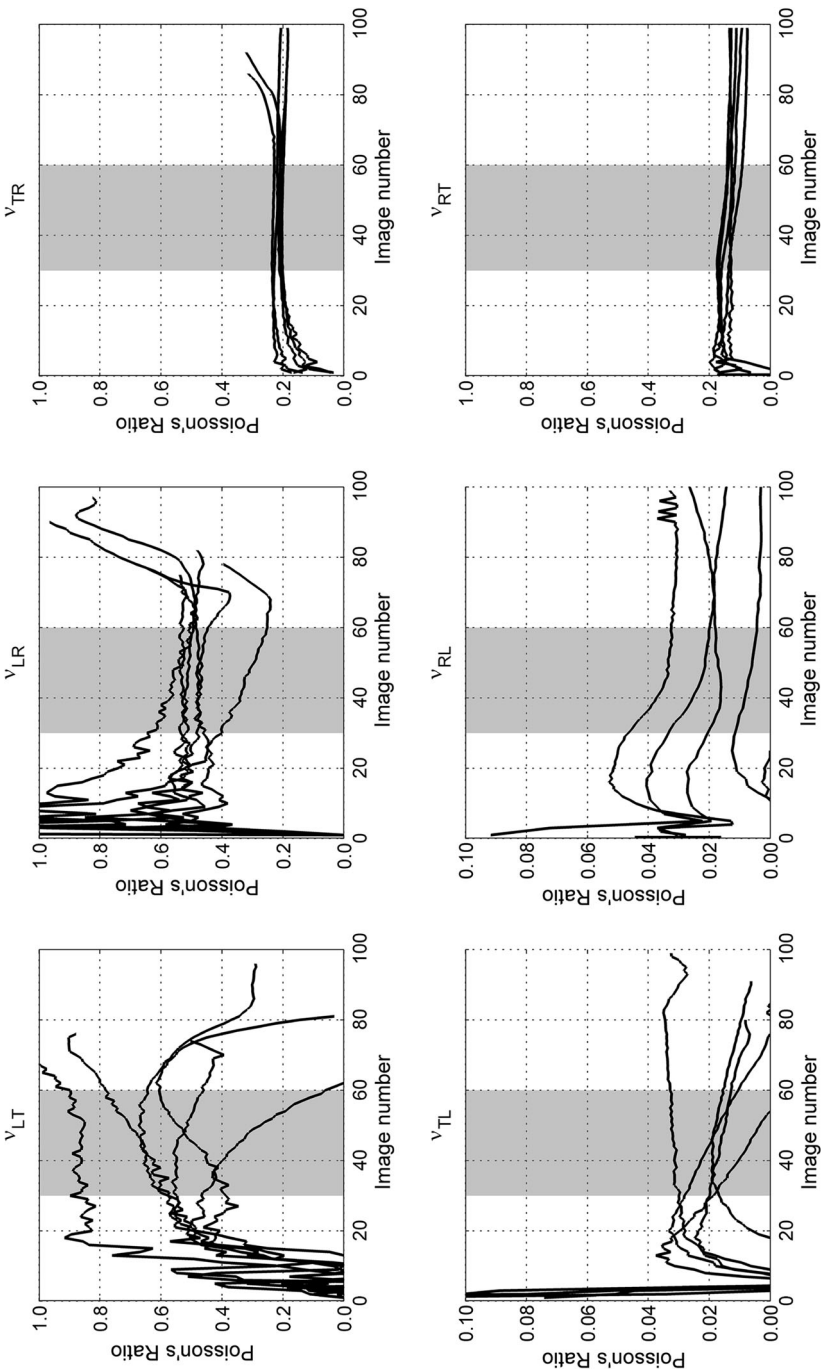

Fig. 4 Evaluation of the six Poisson's ratios of LVL using digital image correlation software

results as fully integrated elements. One edge of the steel plate was loaded with a concentrated force of, respectively, 20 and 80 kN. This edge was restrained against movement perpendicular to direction of loading. The opposite steel plate had one restraint in direction of load and one perpendicular to direction of load.

$$f_v = \frac{F_{max} \times \cos 14^\circ}{lb} \tag{3}$$

Figure 5 shows that shear stress distribution along the centre cross-section is not constant, but is highest in the middle 60 % of the specimen and drops to zero at both ends, which should be the case as there cannot be shear stresses at outside faces. From this model, it follows that maximum actual shear stress in the specimen is 1.22 times the average shear stress. Therefore, when calculating the shear stress based on experimental testing this should be multiplied by a correction factor of 1.22. A very similar shear distribution has been found by Hassel et al. (2009). The almost uniform shear stress distribution found by Sretenovic et al. (2004) could not be reproduced.

The shear strain has been obtained using the DIC technique. Images were taken of each specimen at 5 second intervals until failure of the specimen. Using software, a grid of markers was placed over the centre section of the specimen (Fig. 6a) and markers were tracked through the series of images. An example of the displaced shape, multiplied with a factor 20, is shown in Fig. 6b. For each of the images, the horizontal and vertical shear deformations have been analysed. These deformations

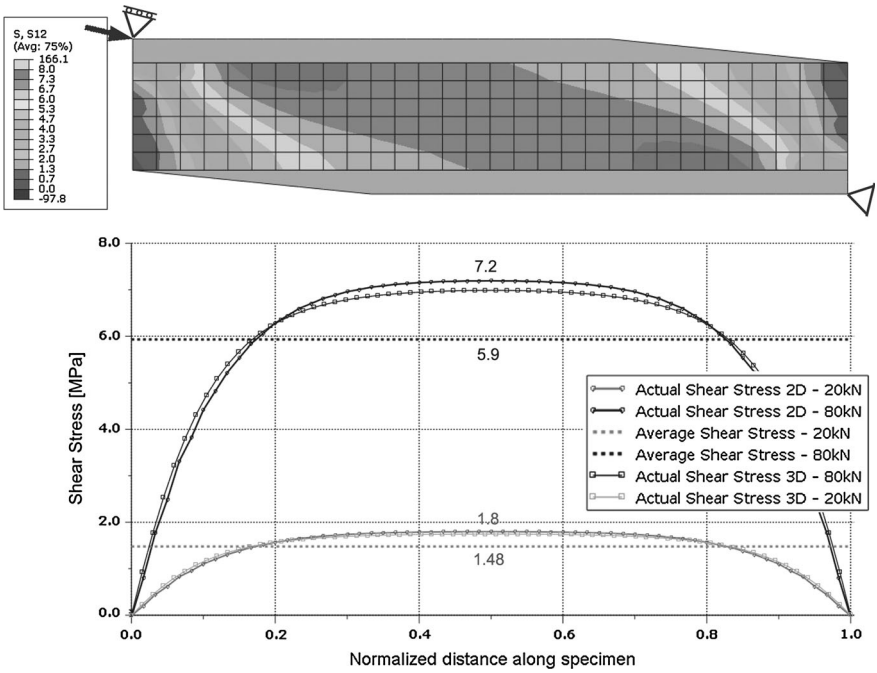

Fig. 5 FEM model of shear test

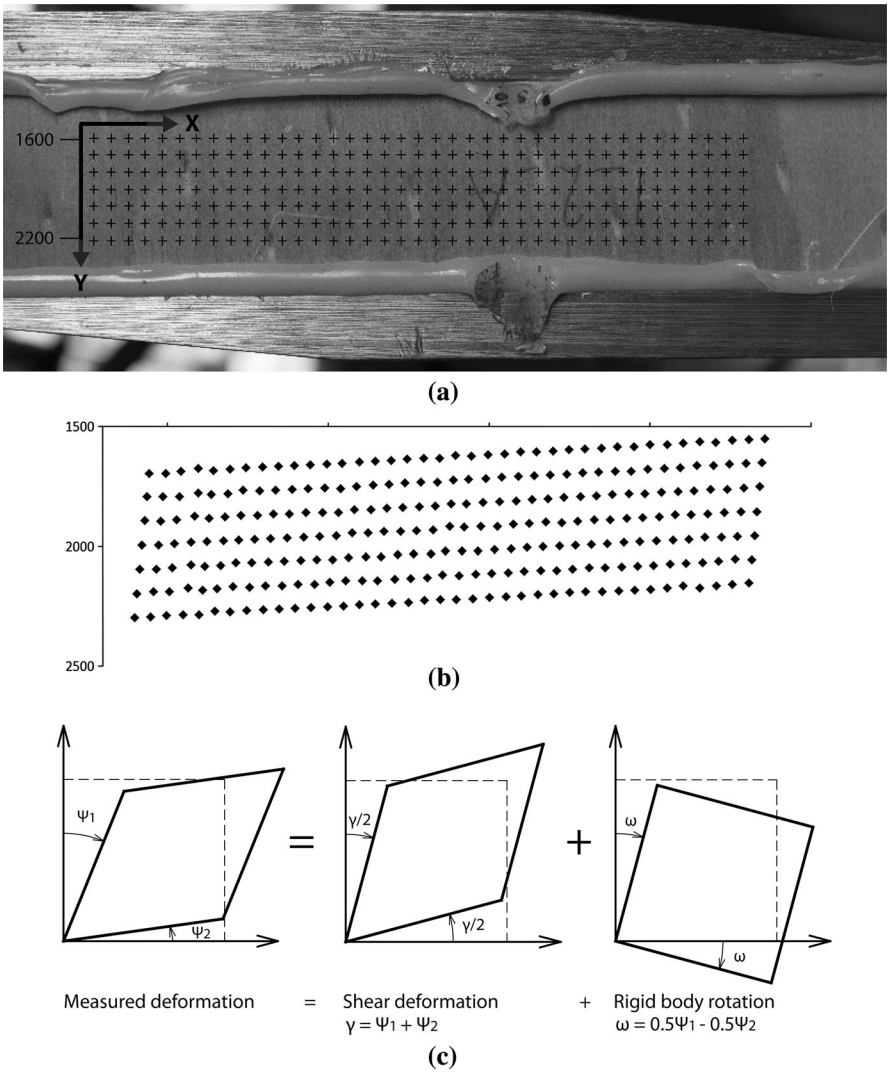

Fig. 6 Evaluation of shear strain using digital image correlation. **a** Specimen (G_{LT}) with generated grid, **b** deformed grid (deformations multiplied by 20), **c** converting measured values into shear deformation and rigid body rotation

have been added to get the total shear deformation (Fig. 6c), and rigid body rotation has been removed. When analysing this for all images the shear strain during testing can be found. Using timestamp of the images and timestamp of loading data, a stress–strain graph can be plotted. The slope of this graph, taken between 10 and 40 % of maximum shear stress, gives the shear modulus. This procedure has been performed for all 36 shear tests, the result of which can be seen in Fig. 7.

Results and discussion

The average and coefficient of variation values for the moduli of elasticity (E), Poisson's ratios (v) and shear moduli (G) in the three material orientations are shown in Table 4. Values of E and G have been calculated using a lognormal distribution as outlined in AS/NZS 4357.3:2006 (Standards New Zealand 2006).

As expected for timber, the stiffness values parallel to grain were much higher than the stiffness perpendicular to grain. The measured value of E_{L} of 12.2 GPa is larger than the specified E of 11 GPa. This is to be expected as the E in compression is higher than the E in bending, and also because the E in bending includes shear deformation (Nelson Pine Industries Limited 2010). The stiffness in the tangential direction was slightly higher than in the radial direction. Variations in stiffness were less than 10 % for all three directions. It should be kept in mind that this is the material variability within one batch of LVL and is not representive of the variability within the LVL product.

The Poisson's ratio is strongly dependent on the direction, as is common for an orthotropic material. The variation in measurements is highest when extension happens in the longitudinal direction, v_{TL} and v_{RL}. This is due to small stresses in this direction and a high modulus of elasticity, resulting in very small strains. The second part of Table 4 shows average and coefficient of variation for off-diagonal terms in the compliance matrix. Normally, this matrix is assumed symmetrical, something which can now be verified. For that a t test has been used to determine if sets of two non-diagonal terms (independent samples with unequal variances) are statistically different. Although timber material properties are assumed to have a lognormal distribution, the skewness of the test data was sufficiently small to use a normal distribution. When comparing v_{LT}/E_L and $v_{\mathrm{TL}}/E_{\mathrm{T}}$ the T value equals 0.16, for v_{LR}/E_{L} and v_{RL}/E_{R} the T value equals 0.79 and for $v_{\mathrm{TR}}/E_{\mathrm{T}}$ and $v_{\mathrm{RT}}/E_{\mathrm{R}}$ the T value equals 7.03. For most comparisons a total of 10 specimens were available, resulting in 8 degrees of freedom. The probabilities corresponding to the T values of 0.16, 0.79 and 7.03 are 88, 45 and 0.01 %, respectively. This indicates a very good correspondence for the first test, a reasonable correspondence for the second test and a very certain difference for the last test. Bodig and Jayne (1982) have also verified symmetry of the compliance matrix. Their conclusion was that although deviations exist the assumption of symmetry holds reasonably well. Furthermore, they note that v_{TL} and v_{RL} are nearly always quite small and may be subject to large experimental error, which has also been the case here. Although some difference between non-diagonal terms is measured, it would have large implications when implementing this in FEM software. Therefore, it is suggested to use Poisson's ratios with the lowest variation: v_{LT}, v_{LR} and v_{TR}.

The shear moduli found under six different loading orientations are listed in Table 4. It can be seen that there is a very good correspondence between G_{LT} and G_{TL}. This should be the case as they correspond to loading in orthogonal plains which result in the same shear stress distribution and thus should result in the same shear stiffness. In addition, the rolling shear moduli, G_{TR} and G_{RT}, are very similar. Only G_{LR} and G_{RL} show a larger difference. In the final part of Table 4, experimental results of orthogonal plains have been averaged. These values show a

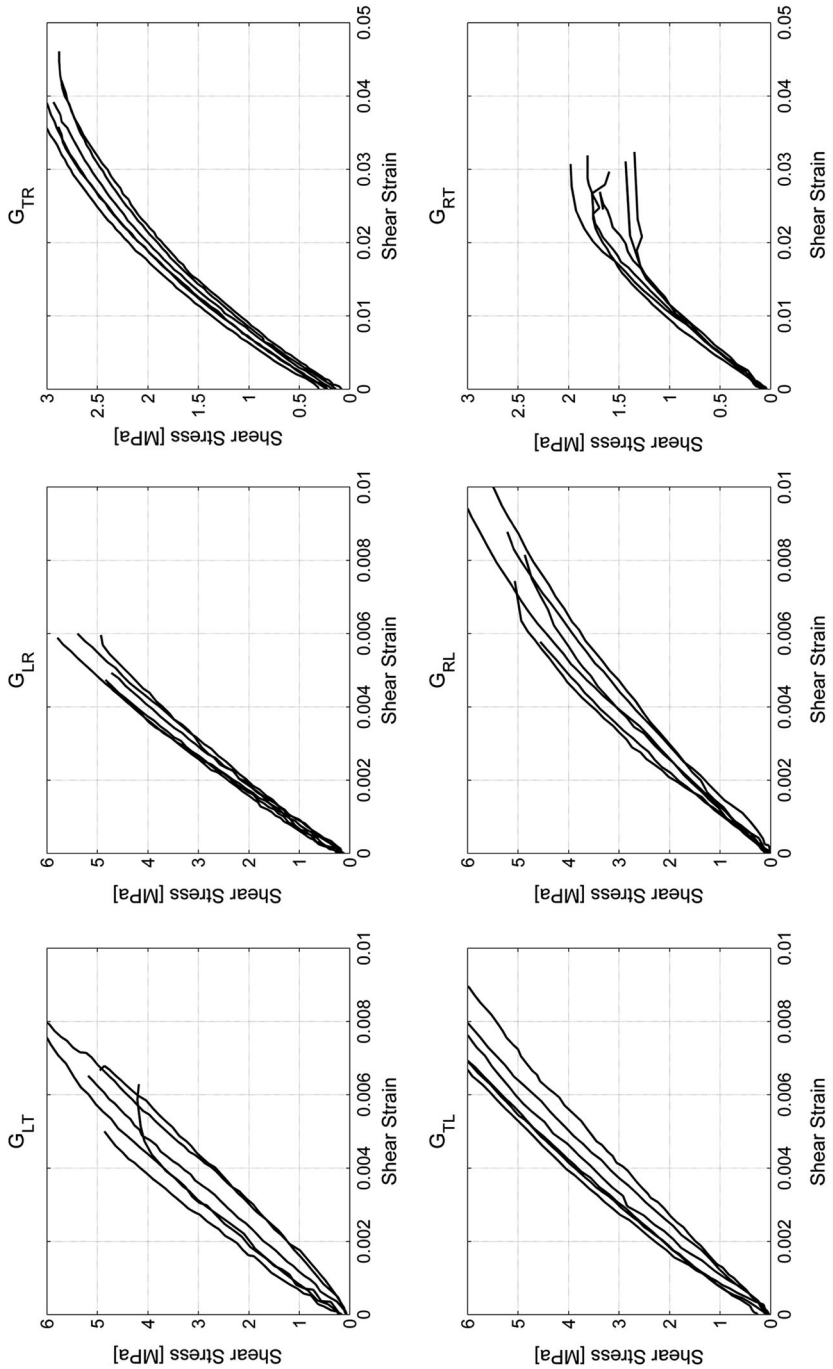

Fig. 7 Shear stress versus shear strain for six different directions

Table 4 Experimental and computed average values and coefficient of variations (CoV) for E, v and G

Property	Average	CoV (%)
$\boldsymbol{E_{\mathrm{L}}}$	**12157 MPa**	7.3
$\boldsymbol{E_{\mathrm{T}}}$	**426 MPa**	5.0
$\boldsymbol{E_{\mathrm{R}}}$	**371 MPa**	8.6
$\boldsymbol{v_{\mathrm{LT}}}$	**0.59**	32.4
v_{TL}	0.02	38.0
$\boldsymbol{v_{\mathrm{LR}}}$	**0.48**	17.6
v_{RL}	0.02	70.3
$\boldsymbol{v_{\mathrm{TR}}}$	**0.22**	5.4
v_{RT}	0.14	12.8
G_{LT}	842 MPa	14.3
G_{TL}	870 MPa	11.8
G_{LR}	1015 MPa	8.3
G_{RL}	786 MPa	14.9
G_{TR}	103 MPa	4.0
G_{RT}	89 MPa	10.8
v_{LT}/E_L	48×10^6	29.4
v_{TL}/E_T	47×10^6	40.6
v_{LR}/E_L	39×10^6	16.3
v_{RL}/E_R	54×10^6	70.9
v_{TR}/E_T	516×10^6	2.6
v_{RT}/E_R	377×10^6	10.8
$\boldsymbol{G_{\mathrm{LT+TL}}}$	**856 MPa**	13.2
$\boldsymbol{G_{\mathrm{LR+RL}}}$	**901 MPa**	18.0
$\boldsymbol{G_{\mathrm{TR+RT}}}$	**96 MPa**	10.8

Bold values are recommended for use in FEM software

variation between 10 and 18 %, indicating good repeatability in testing and analysis procedures.

When comparing experimental results with literature values, shown in Table 1, several conclusions can be drawn. The modulus of elasticity in the longitudinal and the tangential direction (E_{L} and E_{T}) are within range of literature data. Though in the radial direction (E_{R}) the value is lower than all literature values. For sawn timber the modulus of elasticity in the radial direction is always larger than in tangential directions, but this does not seem to be the case for LVL. This was most likely due to stiffer and weaker layers sharing the load perpendicular to grain, whereas the weakest layers are governing the stiffness in the radial direction. On the contrast, for sawn timber stiffness in radial direction is higher than stiffness in tangential direction due to wood rays, which act as reinforcing rods in the radial direction (Wangaard 1979). Due to peeling and glueing of LVL, these rays are most likely damaged and do not contribute to the increased strength and stiffness in radial direction. The glue layers could also have contributed to the increased stiffness in tangential direction. Comparison of E_{R} with other LVL products is not possible as

Janowiak et al. (2001) based modulus of elasticity values on five-point bending tests and thus could not evaluate the radial direction.

The Poisson's ratio ν_{LT} found by experimental testing of 0.59 corresponds well with values for other LVL products found by Janowiak et al. (2001), but within the literature data, there is a large spread in this Poisson's ratio. The Poisson's ratios ν_{LT} and ν_{LR} of Radiata Pine LVL are larger than of sawn pine species. The two small Poisson's ratios, ν_{TL} and ν_{RL}, of 0.02 are within range of literature data. The values of ν_{TR} and especially ν_{RT} are below values mentioned in literature. This can be due to influence of gluelines which add stiffness and reduce strains in tangential direction.

The shear moduli G_{LT} and G_{LR} of 856 and 901 MPa, respectively, are similar to values found in literature for softwoods. Shear stiffness values of different types of LVL, published by Janowiak et al. (2001), are lower than values found for Radiata Pine LVL and also mostly lower than other published values. For most species G_{LR} is slightly higher than G_{LT}, which is also found for Radiata Pine LVL. The rolling shear modulus, G_{TR} of 96 MPa is within range of values reported in literature.

Conclusion

An experimental testing campaign has provided elastic material properties for New Zealand Radiata Pine LVL. Block compression testing in three different material directions has resulted in moduli of elasticity of 12,157, 426 and 371 MPa in longitudinal, tangential and radial directions, respectively. It has been found that modulus of elasticity in the radial direction is lower than in the tangential direction, which is in contrast with literature values of sawn timber. The use of digital cameras and DIC has made it possible to extract Poisson's ratios during the same tests. Poisson's ratios compare well with values of other LVL products found in literature, but differ from literature values of sawn timber. Shear moduli have been determined using DIC on testing according to the European timber testing standard. Values of 856 MPa and 901 MPa have been found for longitudinal shear moduli and 96 MPa for the rolling shear modulus. These results are in line with literature values for sawn timber, but higher than those for LVL manufactured from different species.

The use of DSLR cameras for DIC has proven to give very satisfactory results, although accuracy for two Poisson's ratios was limited due to very small strains along the grain direction whereby variations of up to 70 % were found. Variation in results for moduli of elasticity was less than 9 % and for shear moduli less than 17 %. For most tests, only six specimens were tested, a larger sample size would improve the statistical basis.

The reported elastic material properties make it possible to generate the constitutive matrix needed for FEM analysis. Diagonal terms follow directly from moduli of elasticity and shear moduli. Non-diagonal terms, calculated using Poisson's ratios and moduli of elasticity, are not all symmetrical, but for practical purposes, assumptions can be made to keep the benefits of a symmetrical constitutive matrix.

Acknowledgments LVL used for experimental testing was supplied by Nelson Pine Industries Ltd. Thanks to Alan Poynter for helping out with the test setup and instrumentation of compression tests and to Andrew Dunbar for help with shear testing. Financial support of Structural Timber Innovation Company (STIC) is greatly appreciated. Development of DIC MATLAB software by C. Eberl and his team from Karlsruhe Institute of Technology has been vital to this publication, and their work and the free online access to this software have been very much appreciated.

References

ASTM (2009) D143–09 standard test methods for small clear specimens of timber

ASTM (2010) E132–04 standard test method for Poisson's ratio at room temperature

Bodig J, Goodman JR (1973) Prediction of elastic parameters for wood. Wood Sci 5(4):249–264

Bodig J, Jayne B (1982) Mech Wood Wood Compos. Van Nostrand Reinhold Company, New York

Brandner R, Freytag B, Schickhofer G (2008) Determination of shear modulus by means of standardized four-point bending tests. In: CIB-W18, St. Andrews, Canada, 41–21-1

Buchanan A (2007) Timber design guide, 3rd edn. New Zealand Timber Industry Federation, Wellington

Buchanan A, Palermo A, Carradine D, Pampanin S (2011) Post-tensioned timber frame buildings. Struct Eng 89(17)

Bucur V (2006) Acoustics of wood, 2nd edn. Springer Series in Wood Science, Springer, Berlin

Dahl K, Malo K (2009) Linear shear properties of spruce softwood. Wood Sci Technol 43:499–525

Denzler J, Glos P (2007) Determination of shear strength values according to EN 408. Mater Struct 40:79–86

Divos F, Tanaka T, Nagao H, Kato H (1998) Determination of shear modulus on construction size timber. Wood Sci Technol 32:393–402

Dunbar A, van Beerschoten W, Carradine D (2011) Shear strength and modulus testing of New Zealand laminated veneer lumber. University of Canterbury, Christchurch, Final year project

EN 14374 (2004) Timber structures—structural laminated veneer lumber—requirements. CEN, Brussels

EN 408 (2010) Timber structures—Structural timber and glue laminated timber—determination of characteristic values of mechanical properties and density. CEN, Brussels

Forest Products Laboratory USDA Forest Service (1979) Wood: its structure and properties. Pennsylvania State University

Garab J, Keunecke D, Hering S, Szalai J, Niemz P (2010) Measurement of standard and off-axis elastic moduli and poisson's ratios of spruce and yew wood in the transverse plane. Wood Sci Technol 44(3):451–464

Goncalves R, Trinca A, Cerri D (2011) Comparison of elastic constants of wood determined by ultrasonic wave propagation and static compression testing. Wood Fiber Sci 43(1):64–75

Görlacher R, Kürth J (1994) Determination of shear modulus. In: CIB-W18, Sydney, Australia, 27–10-1

Gunnerson R, Goodman J, Bodig J (1973) Plate test for determination of elastic parameters of wood. Wood Sci 5(4):241–248

Hassel B, Berard P, Modén C, Berglund L (2009) The single cube apparatus for shear testing—full-field strain data and finite element analysis of wood in transverse shear. Compos Sci Technol 69(7):877–882

Hearmon R (1948) Elasticity of wood and plywood, forest products research special report number, seven edn. His Majesty's Stationery Office, London

Janowiak J, Hindman D, Manbeck H (2001) Orthotropic behavior of lumber composite materials. Wood Fiber Sci 33(4):580–594

Ling H, Samarasinghe S, Kulasiri G (2009) Modelling variability in full-field displacement profiles and Poisson ratio of wood in compression using stochastic neural networks. Silva Fenn 43(5):871–887

Nelson Pine Industries Limited (2010) Nelson Pine LVL11—NZ. Technical report NPIL/LVL 04, Nelson Pine Industries Limited, Richmond, Nelson

Niemz P, Caduff D (2008) Untersuchungen zur Bestimmung der poissonschen Konstanten an Fichtenholz. Holz Roh-Werkst 66(1):1–4

Palermo A, Pampanin S, Buchanan AH, Newcombe MP (2005) Seismic design of multi-storey buildings using Laminated Veneer Lumber (LVL). In: New Zealand society for earthquake engineering conference, Taupo

Pan B, Qian K, Xie H, Asundi A (2009) Two-dimensional digital image correlation for in-plane displacement and strain measurement: a review. Meas Sci Technol 20(6):17

Sliker A (1972) Measuring Poisson's ratios in wood. Exp Mech 12(5):239–242

Sretenovic A, Müller U, Gindl W, Teischinger A (2004) New shear assay for the simultaneous determination of shear strength and shear modulus in solid wood finite element modeling and experimental results. Wood Fiber Sci 36(3):302–310

Standards New Zealand (1992) AS/NZS 4063:1992 timber—stress-graded—In-grade strength and stiffness evaluation, Standards New Zealand, Wellington, New Zealand

Standards New Zealand (2006) AS/NZS 4357.3:2006 structural laminated veneer lumber (LVL)—part 3: determination of structural properties—evaluation methods, Wellington

Ukyo S, Ido H, Nagao H, Kato H (2010) Simultaneous determination of shear strength and shear modulus in glued-laminated timber using a full-scale shear block specimen. J Wood Sci 56(3):262–266

US Department of Agriculture Forest Products Laboratory (1955) Wood handbook. Government Printing Office, USA

van Beerschoten W, Palermo A, Carradine D, Sarti F, Buchanan A (2011a) Experimental investigation on the stiffness of beam-column connections in post-tensioned timber frames. In: Structural engineering world conference, Como, Italy, p 12

van Beerschoten W, Smith T, Palermo A, Pampanin S, Ponzo F (2011b) The stiffness of beam to column connections in post-tensioned timber frames. In: CIB-W18, Alghero, Italy, 44–7-7

van Beerschoten W, Carradine D, Palermo A (2013) Compressive strength and stiffness of Radiata Pine laminated veneer lumber. Eur J Wood Wood Prod 71(6):795–804

Wangaard F (1950) The mechanical properties of wood. Wiley, New York

Zink A, Hanna R, Stelmokas J (1997) Measurement of Poisson's ratios for yellow-poplar. For Prod J 47(3):78–80